Am J Cancer Res 2021;11(10):4900-4918
www.ajcr.us /ISSN:2156-6976/ajcr0137028

Original Article

Paired-like homeodomain 2B contributes to tumour progression and anti-autophagy in human lung cancer

Chi-Chung Wang[1*], Sheng-Yi Lin[2*], Yu-Han Huang[2], Chia-Hung Hsieh[3], Hsiu-Hui Chang[2], Hsuan-Yu Chen[4], Chia-Wei Weng[2], Gee-Chen Chang[2,5,6], Sung-Liang Yu[7], Jeremy JW Chen[2,8]

[1]Graduate Institute of Biomedical and Pharmaceutical Science, Fu Jen Catholic University, New Taipei, Taiwan; [2]Institute of Biomedical Sciences, National Chung Hsing University, Taichung, Taiwan; [3]Graduate Institute of Biomedical Sciences, China Medical University, Taichung, Taiwan; [4]Institute of Statistical Science, Academia Sinica, Taipei, Taiwan; [5]Division of Pulmonary Medicine, Department of Internal Medicine, Chung Shan Medical University Hospital, Taichung, Taiwan; [6]Division of Chest Medicine, Department of Internal Medicine, Taichung Veterans General Hospital, Taichung, Taiwan; [7]Department of Clinical and Laboratory Sciences and Medical Biotechnology, National Taiwan University College of Medicine, Taipei, Taiwan; [8]Institute of Molecular Biology, National Chung Hsing University, Taichung, Taiwan. [*]Equal contributors.

Received July 5, 2021; Accepted September 19, 2021; Epub October 15, 2021; Published October 30, 2021

Abstract: Paired-like homeodomain transcription factor 2 (*PITX2*) is well known to play an essential role in normal embryonic development. Emerging evidence suggests that *PITX2* may be involved in human tumorigenesis, but the role of *PITX2* in tumour progression remains largely unclear. The expression levels of *PITX2* in lung cancer cells were determined by qRT-PCR and Western blot analyses. Gain- and loss-of-function experiments were conducted to investigate the biological roles of *PITX2* in the phenotype of lung cancer cells. Immunofluorescence staining and transmission electron microscopy were used to observe autophagy. The expression level and clinical significance of *PITX2* were determined in a Taiwanese cohort and the Gene Expression Omnibus (GEO) database, respectively. Here, we show that *PITX2B* is the most abundant isoform of the bicoid homeodomain family in lung cancer cells. The enforced expression of PITX2B promoted lung cancer tumorigenesis and progression *in vitro* and *in vivo*. The mechanistic analysis revealed that the nuclear localization of PITX2B is correlated with its oncogenic functions and two important nuclear localization signals. In addition, *PITX2B* knockdown in lung cancer cells caused a marked increase in autophagy and apoptosis, suggesting that PITX2B plays an important role in lung cancer cell survival. Moreover, a high expression of *PITX2B* was associated with a poor overall survival ($P<0.05$) in both Taiwanese non-small-cell lung cancer patients and GEO lung cancer cohorts. These results provide new insight into the contribution of *PITX2B* to lung cancer progression, implicate PITX2B as an important component of cell survival signals and further establish *PITX2B* as a therapeutic target for lung cancer treatment.

Keywords: PITX2, NSCLC, tumorigenesis, NLS, autophagy

Introduction

Lung cancer is among the most common malignancies worldwide and the leading cause of cancer-related death in many countries, including Taiwan. Among all lung cancer cases, 85% are non-small-cell lung cancer (NSCLC) [1]. Over 75% of lung cancer patients are diagnosed at an advanced or metastatic stage partially due to the lack of an effective screening platform for early detection [2]. Thus, only 12-16% of lung cancer cases are detected early, and the overall five-year survival rate of lung cancer patients is only 19% in the United States of America [3, 4]. Because of the limitations of the current screening techniques and the poor five-year survival rates, the development of improved methods, such as specific and sensitive molecular biomarkers, for the early detection of lung cancer is urgently needed. Recent studies have indicated that several genes, including paired-like homeodomain transcription factor 2 (*PITX2*), show abnormal methylation levels in tumour tissue compared with adjacent nontumour lung tissue and can serve as DNA methylation markers for the early detection of lung cancer [5, 6].

PITX2B is a member of the bicoid homeodomain family and is critical for normal embryonic development in vertebrates [7]. PITX2B is required for the morphogenesis of anterior structures, the establishment of left/right patterning, and the asymmetrical development of multiple organs, including the lungs [8]. Mutations in this gene are associated with the pathogenesis of Axenfeld-Rieger syndrome (ARS), which is an autosomal-dominant disorder predominantly affecting the eyes, teeth, and heart [9]. However, the possible mechanisms of action of PITX2 in human tumour progression have not been completely elucidated. The human *PITX2* gene is represented by four different splicing transcripts, namely, *PITX2A*, *-B*, *-C*, and *-D* [10, 11]. Although the differential functions of the different *PITX2* isoforms during organogenesis have been studied, the exact cellular functions of these *PITX2* isoforms in tumorigenesis remain elusive [12]. Recently, PITX2B was found to be overexpressed in ovarian, thyroid, colon, kidney, lung, and pituitary cancers and to contribute to carcinogenesis by promoting tumour growth and/or suppressing apoptosis [13-18]. However, to date, the role of the *PITX2* isoform *PITX2B* in lung carcinogenesis and progression remains unclear.

Chemotherapy is a critical strategy for controlling or curing lung cancer. Many attempts have been expanded to decrease resistance and improve therapeutic effectiveness. However, the effects of these therapies remain inadequate. Therefore, it is desirable to identify more appropriate therapeutic strategies for NSCLC. Recently, many emerging studies suggested that autophagy may be a novel therapeutic target in the treatment of cancer [19]. Autophagy is an evolutionarily conserved catabolic process that participates in development and differentiation and is essential for growth regulation and the maintenance of homeostasis in various eukaryotes [20, 21]. Although autophagy can be induced by ionizing radiation or chemical agents in many different tumour cell lines, this process seems to play a contradictory role in the regulation of cancer cell survival and death outcomes [22]. Therefore, appropriate autophagy modifications that lead to apoptosis in tumour cells in response to genetic dysfunction or antitumour agents might improve the efficacy of chemotherapy.

In this study, for the first time, we demonstrate the biological functions of *PITX2B*, which is the most abundant isoform of the bicoid homeo domain family in human lung adenocarcinoma cells, and its association with clinical outcomes in NSCLC patients. We found that the overexpression of *PITX2B* could increase migration, invasion, and colony formation capabilities *in vitro* and tumorigenesis *in vivo*. The oncogenic functions of PITX2B were correlated with nuclear PITX2B localization, and two critical nuclear localization signals (NLSs) were identified. Furthermore, a high expression level of *PITX2B* was correlated with reduced overall survival in NSCLC patients. Interestingly, the knockdown of *PITX2B* could potentially induce autophagy and apoptosis in lung adenocarcinoma cells. Our findings provide further insight into the therapeutic role of *PITX2B* in controlling lung cancer tumorigenesis.

Materials and methods

Cell culture and patient specimens

The cell lines CL1-5 and CL1-0 (in descending order of invasive ability; human lung adenocarcinoma cells) were established in our previous study [23]. RPMI 1640 or DMEM (Thermo Fisher Scientific, Inc., Carlsbad, CA, USA) supplemented with 1% penicillin-streptomycin (Thermo Fisher Scientific) and 10% heat-inactivated foetal bovine serum (FBS; Thermo Fisher Scientific) was used to culture all cell lines, including H1755 (ATCC CRL-5892), A549 (ATCC CCL-185), and H1299 (ATCC CRL-5803). The cells were maintained under standard culture conditions of 5% CO_2 and 37°C in a humidified atmosphere incubator. Frozen specimens of lung cancer tissue from 98 early-stage NSCLC patients were collected for a reverse transcription-polymerase chain reaction (RT-PCR) analysis. All patients underwent surgical resection of NSCLC between December 1999 and March 2009 at the Taichung Veterans General Hospital. Among the 98 specimens, 21 were squamous cell carcinomas, and 77 were adenocarcinomas. The institutional review board of the hospital approved this study (IRB TCVGH No: CE14015). Written informed consent was obtained from all patients, and the postsurgical pathologic stage of each tumour was classified according to the international tumour-node-metastasis (TNM) classification [24].

Plasmid construction and transfection

TRIzol reagent (Thermo Fisher Scientific) was used to isolate the total RNA from the CL1-5

cells for the *PITX2B* full-length cDNA identification and cloning. SuperScript II reverse transcriptase (Thermo Fisher Scientific) and oligo-dT primers were used to reverse-transcribe first-strand cDNA products. The coding region of *PITX2B* was amplified by polymerase chain reaction (PCR) using the *PITX2B*-F primer 5'-CGGGATCCATGGAGACCAACTGCCGTAAACTGGTGT-3', which introduced a *Bam*HI site, and the *PITX2B*-R primer 5'-GCTCTAGACTCACGGGCCGGTCCACTGCATACTGGCAA-3', which introduced an *Xba*I site. Then, the amplified PCR product was cloned into a pcDNA3.1-V5-His TOPO vector (Thermo Fisher Scientific; pcDNA3.1-*PITX2B*). To ensure the correction of the cDNA sequences, the cDNA was checked by sequencing. Stable CL1-0/PITX2B-overexpressing or vector control cells were established for the cellular functional analysis. The CL1-0 cells were transfected with the pcDNA3.1-PITX2B or pcDNA3.1 plasmid, and then, stable cell clones were selected with Geneticin (G418; Merck, Darmstadt, Germany) as previously described [25]. In addition, EGFP-tagged *PITX2B* was subcloned into the pEGFP-C3 vector (Clontech, Laboratories, Inc., Mountain View, CA, USA). The NLS mutant constructs pEGFP-C3-PITX2B-R84P, pEGFP-C3-PITX2B-R137P, pcDNA3.1-PITX2B-R84P, and pcDNA3.1-PITX2B-R137P were generated by site-directed mutagenesis, and the mutagenesis primers (the target site of mutagenesis is marked by an underline) were as follows: R84P, forward primer 5'-CGTCTAAGAAGAAGC<u>C</u>GCAAAGGCGGCAGC-3' and reverse primer 5'-GCTGCCGCCTTTGC<u>G</u>GCTTCTTCTTAGACG-3', and R137P, forward primer 5'-GGTTCAAGAATCGTC<u>C</u>GGCCAAATGGAGAAAGAG-3' and reverse primer 5'-CTCTTTCTCCATTTGGCC<u>G</u>GACGATTCTTGAACC-3'. The desired mutations were confirmed by DNA sequencing. The pEGFP-LC3 plasmid was a gift from Karla Kirkegaard (Addgene plasmid #11546; http://n2t.net/addgene:11546; RRID: Addgene_11546). Approximately 2×10^5 cells per well were seeded for 24 h before the transfection. Lipofectamine reagent (Thermo Fisher Scientific) was used to transfect the plasmids into the tested cells according to the manufacturer's protocols.

Real-time quantitative reverse transcription-PCR (qRT-PCR)

TRIzol reagent (Thermo Fisher Scientific) was used to extract the total RNA from the cell lines or patient tissues. To quantify the expression of PITX2 in the clinical specimens, an ABI TaqMan qPCR assay (Hs04234067_g1, Thermo Fisher Scientific) was used, and TATA-box binding protein (TBP; Hs00427620_m1) was used for normalization of gene expression. SYBR Green RT-PCR was performed to examine the *PITX2B* expression levels in the tested cell lines. The primer sets designed for various *PITX2* isoforms were as follows: *PITX2A*, forward primer 5'-GCGTGTGTGCAATTAGAGAAAG-3' and reverse primer 5'-TTCCTCTGGAAAGTGGCCTC-3'; *PITX-2B*, forward primer 5'-GCAGCCAGCAGCAAGTTCTT-3' and reverse primer 5'-GCTGCTGGCTGGTAAAGTGAG-3'; and *PITX2C*, forward primer 5'-GAGGTGCACACCATCTCCGA-3' and reverse primer 5'-GCTGCTGGCTGGTAAAGTGAG-3'. TBP was quantified as an internal control (GenBank X54993).

Western blot analysis

A Western blot analysis was performed to determine the protein expression levels of the target genes in various cell lines or after different treatments. The procedures were carried out as previously described [25]. The primary antibodies against PITX2 (Santa Cruz Biotechnology, Santa Cruz, CA, USA, sc-8748), LC3 (Novus, Inc., Littleton, CO, NB100-2220), p62 (Novus, Inc., Littleton, CO, USA, NBP1-48320), Beclin-1 (Novus, Inc., Littleton, CO, USA, NB-110-87318SS), Bcl-2 (Upstate Biotechnology, Lake Placid, NY, USA, 05-826), Caspase 3 (Chemicon, CA, USA, AB1899) and PARP (Cell Signalling Technology, Danvers, MA, USA, 95-42) were diluted from 1:1,000 to 1:3,000. The anti-V5 antibody was purchased from Thermo Fisher Scientific, Inc. (R960-25, Carlsbad, CA, USA), and β-tubulin (Upstate Biotechnology, Lake Placid, NY, USA, 05-661) was used as an internal control. The membranes were incubated overnight with the primary antibodies. Subsequently, the blots were washed and incubated with a horseradish peroxidase (HRP)-conjugated secondary antibody (Santa Cruz Biotechnology, Santa Cruz, CA, USA). The blots were detected using an enhanced chemiluminescence system (ECL, GE Healthcare, Piscataway, NJ, USA).

Migration and invasion assays

The migratory capability of the *PITX2B* transfectants or mock control transfectants was evaluated using wound healing assays [25].

The number of cells that migrated into the cell-free zone was counted. The invasiveness of the CL1-0 cells transfected with the vector alone or *PITX2B* expression plasmid was evaluated using Transwell chambers and Matrigel (BD Biosciences, Franklin Lakes, NJ, USA)-coated Transwell filters (8-μm pore size; Corning Costar, Cambridge, MA, USA) [25]. The cells that migrated to the lower surface of the polycarbonate filter were fixed, stained, and counted under a light microscope. All experiments were performed three times in triplicate.

Clonogenic assay and in vivo tumorigenesis assay

For the anchorage-dependent colony formation assay, 500 cells were resuspended in DMEM and seeded in six-well plates for one week. For the anchorage-independent colony formation assay, 500 cells were seeded and treated according to previously described procedures [25]. The experiments were performed three times in duplicate. For the animal study, six-week-old nude mice were purchased from the National Laboratory Animal Center of Taiwan and used as xenograft tumour models. All animals were housed in a specific pathogen-free (SPF) environment, and the Institutional Animal Care and Use Committee of National Chung Hsing University approved all *in vivo* experiments. For the *in vivo* tumorigenesis assay, to avoid individual clonal differences, 3×10^6 pooled *PITX2B* transfectants (PITX2B-Mix) or mock control transfectants were injected subcutaneously into the dorsal region of the nude mice. The body weights and tumour sizes were recorded twice weekly, and the mice were observed regularly. The mice were sacrificed at 50 days, and the tumours were removed, weighed, and imaged. Callipers were used to measure the length and width of the tumour samples. The following formula was used to calculate the tumour volume (TV): TV (mm^3) = (length × $width^2$) ×0.5.

Cell viability and autophagy evaluation

To study the effect of a decreased *PITX2B* expression on cell viability and autophagy, a gene silencing strategy was employed in this study. For the small interfering RNA (siRNA) transient transfection, 2 sets of desalted siRNA duplexes, 5'-CCAGGCTATTCCTACAACA-3' and 5'-ACTCCTCCGTATGTTTATA-3', were synthesized (Qiagen, Hilden, Germany) and annealed according to the manufacturer's instructions. RNAiFect Transfection Reagent (Qiagen, Hilden, Germany) was used to perform the *PITX2*-specific and scrambled control siRNA transfection. Western blot and real-time RT-PCR analyses were used to examine the efficacy of the siRNAs. The cell viability was determined by counting CL1-5 cells and *PITX2*-specific or scrambled siRNA-transfected cells (seeded at 1×10^5 cells/well in 6-well plates) for 3 days after the siRNA transfection using a trypan blue staining protocol. The experiments were performed three times in duplicate. In addition, to confirm the effects of *PITX2B* on the viability of the CL1-5 cells, two *PITX2*-specific short hairpin RNAs (shRNAs) designated pLKO.1-sh*PITX2*-G1 (TRCN0000235580) and pLKO.1-sh*PITX2*-B2 (TRCN0000235581) and lacZ control shRNA (pLKO.1-shLacZ, TRCN0000072224) lentiviral vectors were obtained from the National RNAi Core Facility (Academia Sinica, Taiwan). The CL1-5 cells were infected with lentivirus in medium containing polybrene (8 μg/ml). After infection for 24 h, the cells were treated with 2.5 μg/ml puromycin for 3-7 days. For the autophagy inhibitor treatment experiment, the tested cells were treated with 100 μM NH_4Cl after the siRNA transfection for 24 h.

Transmission electron microscopy (TEM)

After the CL1-5 cells were transfected with *PITX2*-specific or scramble siRNA for 48 h, the cells were washed and collected by centrifugation. The cells were fixed in ice-cold 4% paraformaldehyde and 2.5% glutaraldehyde, postfixed in 1% osmium tetroxide, dehydrated with ethanol (30%-100%), and then embedded in Spurr's resin for sectioning. Ultrathin sections (70 nm) were prepared, double stained with lead citrate and uranyl acetate and examined under a JEM-1400 transmission electron microscope (JEOL, USA).

Immunofluorescence staining

The BEAS2B-EGFP-LC3 cells were gifts from Prof Jeng Jer Shieh at the Institute of Biomedical Sciences, National Chung Hsing University, Taichung, Taiwan. The BEAS2B-EGFP-LC3 cells were seeded on glass coverslips. After the transfection with *PITX2*-specific or scramble siRNAs, the cells were fixed with 4% paraformaldehyde and washed with PBS; then, the

EGFP-LC3 puncta were examined under a fluorescence microscope (Olympus BX51, Olympus Co., Tokyo, Japan). For the cellular PITX2B localization analysis, EGFP-*PITX2B* or NLS mutant construct-transfected cells cultured on 12-mm glass coverslips were fixed with 4% paraformaldehyde, permeabilized, and then stained. F-actin filaments were stained with TRITC-conjugated phalloidin, and 4',6-diamino-2-phenylindole (DAPI) was used to counterstain the cellular nuclei. Images were acquired under a fluorescence microscope (Olympus BX51). The contrast, colour balance, final image size, and brightness were adjusted using Adobe Photoshop CS2.

Survival analyses using gene expression and clinical data

To evaluate the effect of the PITX2 expression levels on clinical prognosis, six published microarray datasets comprising 982 lung cancer patients were collected from the Gene Expression Omnibus (GEO) database under accession numbers GSE30219 [26], GSE37745 [27-29], GSE29013 [30], GSE31210 [31, 32], GSE50081 [33], and GSE31546. The clinical data were obtained from the GEO Series Matrix files. The pathologic stage of each sample was checked according to the international TNM classification [24]. To reduce variation among the microarrays, a quantile normalization method [34] was used to rescale the intensity values of the samples in each microarray. Subsequently, each intensity value was log-transformed to a base-2 scale. Then, the early-stage NSCLC samples (stage I + stage II; n= 736) were extracted from the original specimens for the survival analysis. Furthermore, the *PITX2* expression levels obtained from recruited Taiwanese patients with early-stage NSCLC (stage I + stage II; n=98) were employed to assess the clinical outcome. The patients were stratified into high and low *PITX2* expression groups. The log-rank test was performed to evaluate the difference between the two groups, and the Kaplan-Meier method was used to assess overall survival. The independent prognostic factors were evaluated using a multivariate Cox proportional hazards regression analysis, and age and sex were used as covariates. All analyses were performed using SAS version 9.1 software (SAS Institute, Cary, NC, USA).

Statistical analysis

The significant differences in all *in vitro* experiments were determined using an ANOVA (Excel, Microsoft). All statistical tests were two-tailed, and $P<0.05$ was considered statistically significant. Where appropriate, the data are presented as the mean ± SD.

Results

Expression pattern and impact of PITX2B on lung cancer cell morphology

Although the functional roles of *PITX2* during embryogenesis have been extensively studied, the role of *PITX2* isoforms in human lung cancer is barely understood. There are three major *PITX2* isoforms with intact homeodomains in the human genome [35]. Here, we first identified the dominant *PITX2* isoform in human lung cancer cells by using qRT-PCR. We found that the mRNA level of *PITX2B* was significantly increased in two human lung adenocarcinoma cell lines, namely, CL1-5 and CL1-0 (**Figure 1A**). In contrast, the *PITX2* isoforms *PITX2A* and *PITX2C,* which were previously studied in great detail, were rarely expressed in our tested cells. We established a series of human lung adenocarcinoma cell lines with various invasive capabilities in our previous studies [25, 36]. In these cell lines, the mRNA expression of *PITX2B* in the less invasive CL1-0 cells was lower than that in the highly invasive CL1-5 cells. Thus, the expression of *PITX2B* seems to be positively associated with the cell invasive ability. Then, we detected the expression of *PITX2B* in other lung cancer cell lines, including A549, H1755, and H1299. A high expression of *PITX2B* was observed in these tested lung cancer cells, except for the CL1-0 cells, in which *PITX2B* was expressed at lower levels (**Figure 1B**). CL1-0 cell clones with stable constitutive *PITX2B* expression were established to elucidate the effects of *PITX2B* expression on lung cancer progression. qRT-PCR and Western blot analyses were used to determine the mRNA and protein expression levels of *PITX2B* in these stable cell lines (**Figure 1C** and **1D**). The *PITX2B* transfectants expressed higher levels of the *PITX2B* protein and mRNA than the mock control cells (Mock). One mixed clone (PITX2B-Mix) and three single clones (PITX2B-3, -5, and -7) that stably expressed *PITX2B* were isolated for further studies. Furthermore, after the *PITX2B*

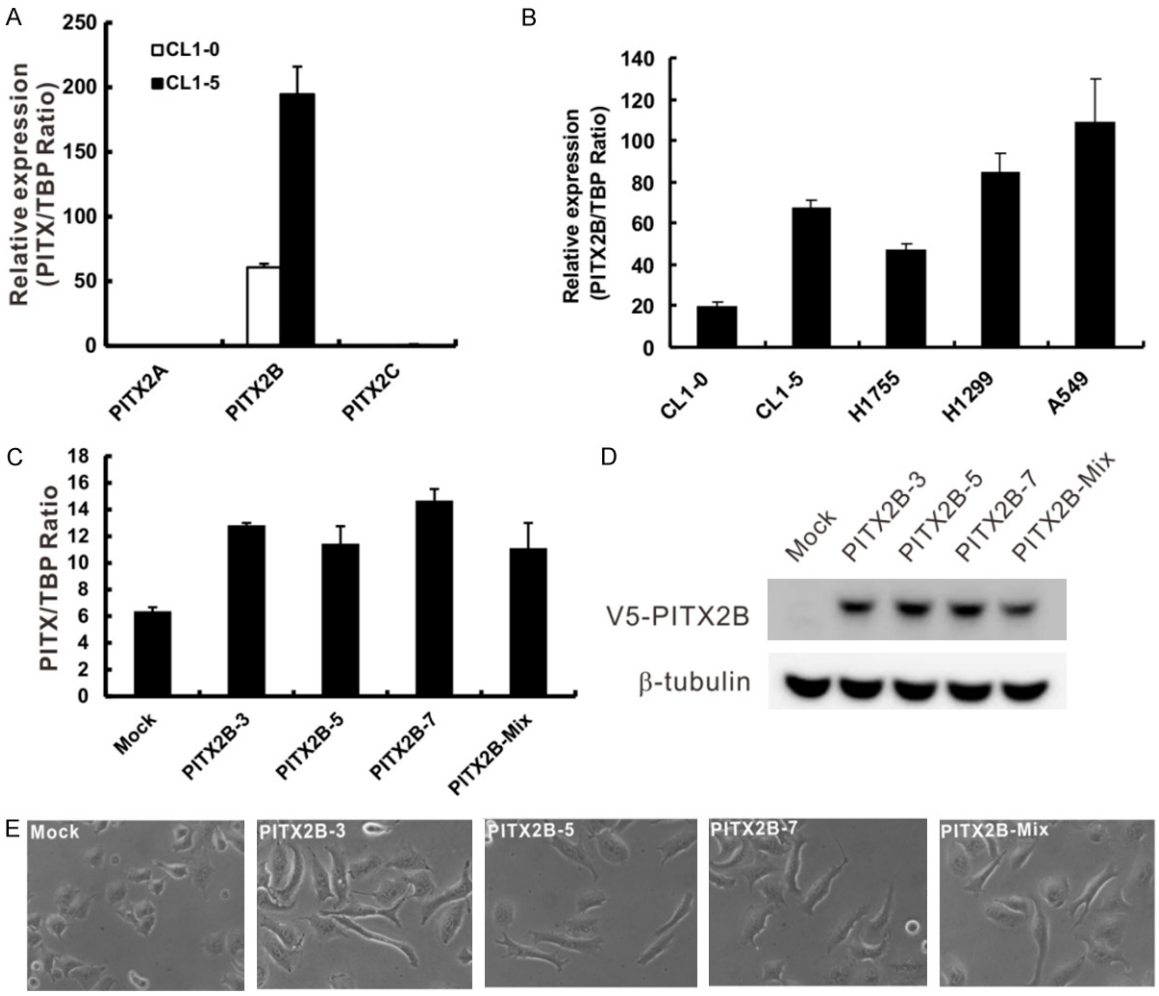

Figure 1. *PITX2B* is the dominant isoform in lung cancer cells and can change the cell morphology. A. mRNA expression levels of different *PITX2* isoforms in lung cancer cell models as assessed by real-time quantitative RT-PCR. The invasive ability of CL1-0 cells is lower than that of CL1-5 cells. B. *PITX2B* mRNA levels in different lung cancer cells as measured by real-time quantitative RT-PCR. All experiments were performed three times in triplicate. C. *PITX2B* mRNA expression in transfected cells with constitutive *PITX2B* expression as measured by quantitative RT-PCR. PITX2B-3, -5, and -7: single-cell clones; PITX2B-Mix: mixed-cell clones; Mock: vector transfectant. TATA-binding protein (*TBP*) was used as an internal control. D. PITX2B protein expression in the transfectants was determined by a Western blot analysis with an anti-V5 antibody. β-Tubulin served as a loading control. E. Cell morphology images of *PITX2B* transfectants and mock stable transfectants. *PITX2B* transfectants exhibit spindle-like shapes, whereas mock transfectants exhibit a rounded morphology.

transfection, the morphology of the CL1-0 cells changed from a rounded, cobblestone appearance and reverted to a spindle-like shape (**Figure 1E**).

PITX2B promotes lung cancer progression

Given that an increased *PITX2B* expression was positively associated with cell invasive capabilities and mesenchymal morphology, we investigated whether *PITX2B* plays a role in promoting migration and invasion in lung cancer cells. The migration ability of the *PITX2B* transfectants was markedly increased compared with that of the mock transfectants (Mock) in the wound healing assay (**Figure 2A**). In addition, in the Transwell invasion assay, we found that the *PITX2B* transfectants exhibited significantly higher invasive capabilities than the mock transfectants (**Figure 2B**). Previous studies have suggested that PITX2 could play some roles in cancer cell proliferation and growth [13, 16]; thus, we performed an *in vitro* anchorage-dependent assay to evaluate the effect of PITX2 on lung cancer cell growth. As shown in **Figure 2C**, the colony formation ability of the *PITX2B* transfectants was significantly increased from 2.5- to 4.7-fold compared with that

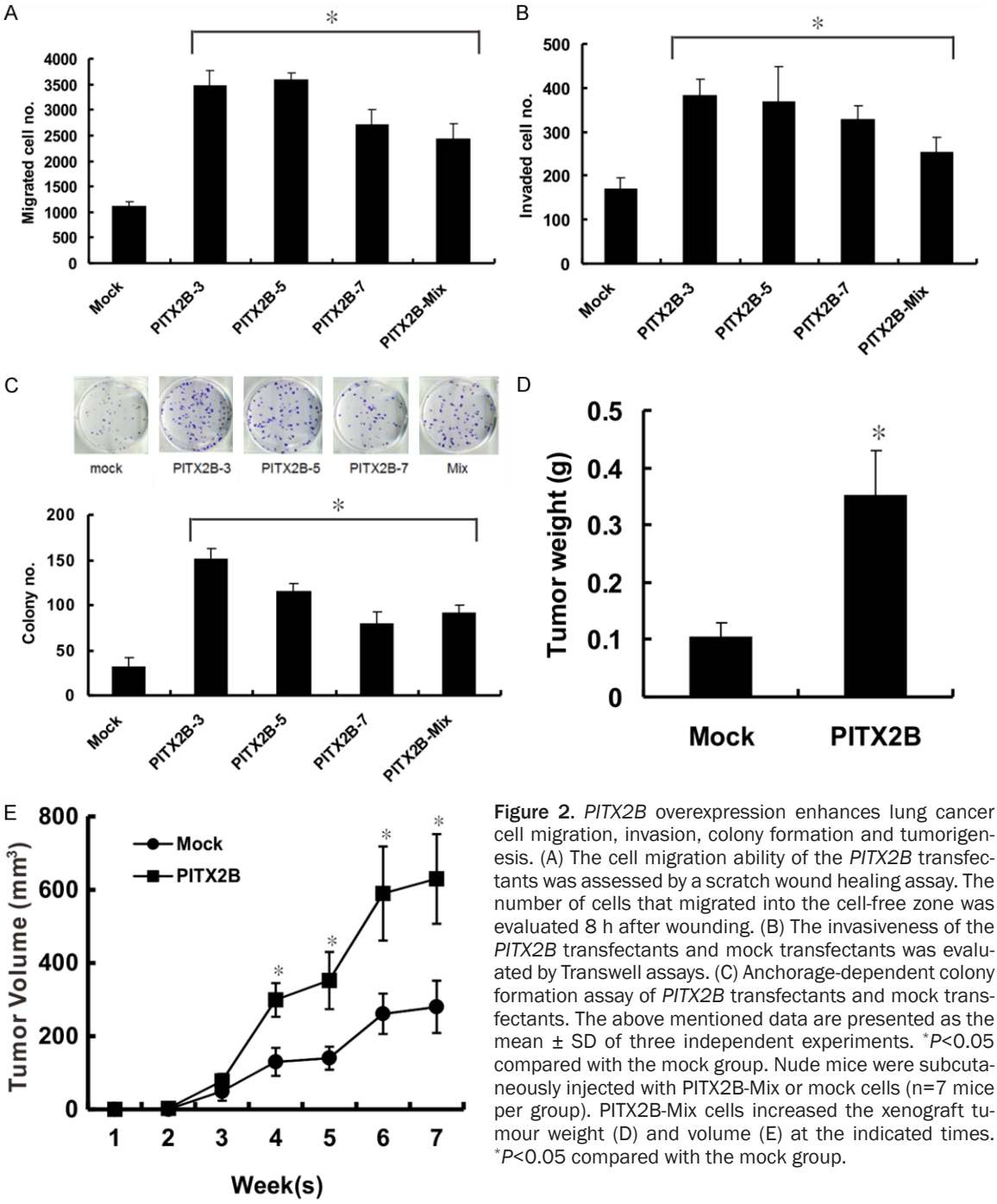

Figure 2. *PITX2B* overexpression enhances lung cancer cell migration, invasion, colony formation and tumorigenesis. (A) The cell migration ability of the *PITX2B* transfectants was assessed by a scratch wound healing assay. The number of cells that migrated into the cell-free zone was evaluated 8 h after wounding. (B) The invasiveness of the *PITX2B* transfectants and mock transfectants was evaluated by Transwell assays. (C) Anchorage-dependent colony formation assay of *PITX2B* transfectants and mock transfectants. The above mentioned data are presented as the mean ± SD of three independent experiments. $^{*}P<0.05$ compared with the mock group. Nude mice were subcutaneously injected with PITX2B-Mix or mock cells (n=7 mice per group). PITX2B-Mix cells increased the xenograft tumour weight (D) and volume (E) at the indicated times. $^{*}P<0.05$ compared with the mock group.

of the mock transfectants. To determine whether the overexpression of *PITX2B* could also enhance tumour growth ability *in vivo*, the PITX2B-Mix clone and mock control cells were inoculated subcutaneously into nude mice. After 50 days, we observed that the PITX2B-Mix clone resulted in 3.4- and 2.2-fold increases in the tumour weight and volume, respectively, compared with the mock control cells (**Figure 2D** and **2E**; $P<0.05$, n=7 in both groups). Taken together, these results suggest that PITX2 expression can promote cancer cell migration, invasion, and growth *in vitro* and tumorigenesis *in vivo*.

NLS is important for PITX2B oncogenic function in lung cancer cells

A previous study demonstrated that the transcriptional activity of *PITX2* may regulate the

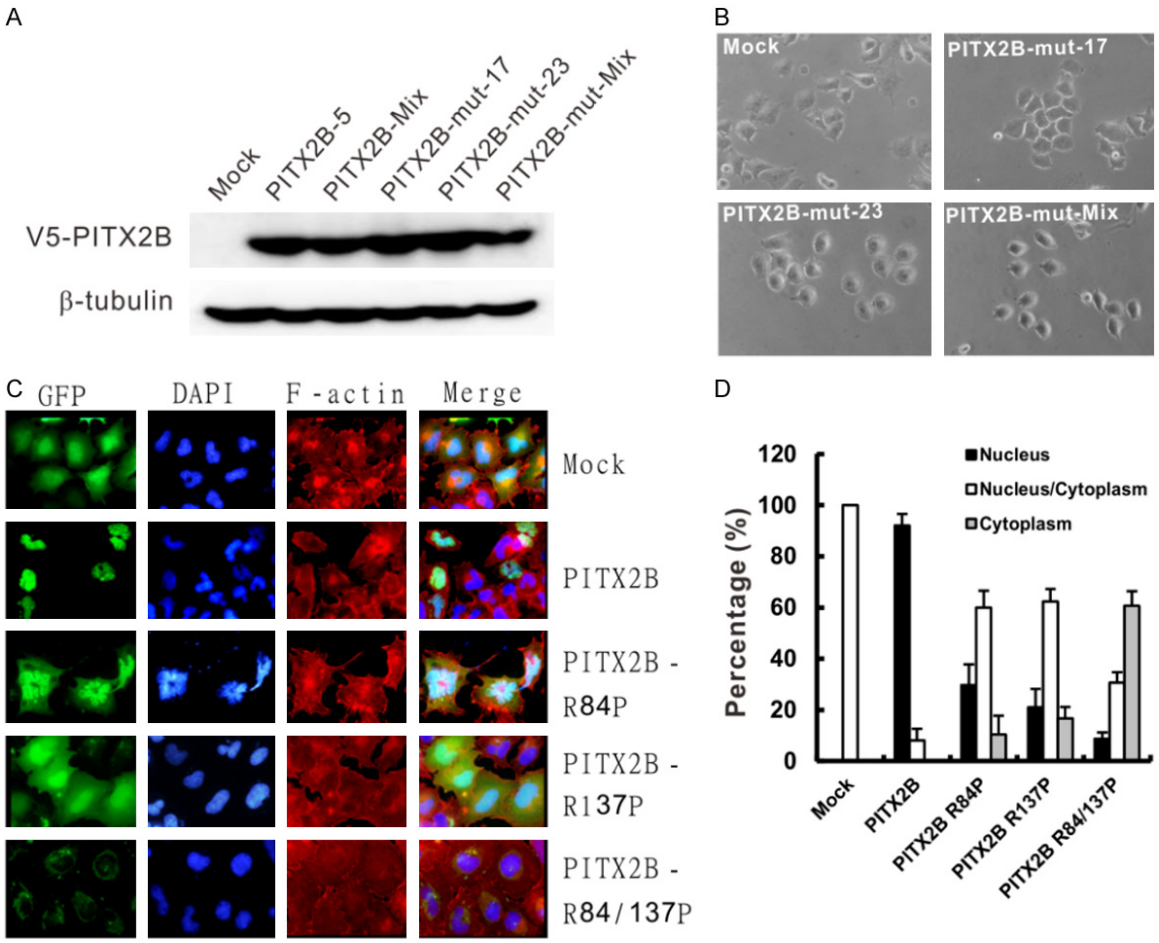

Figure 3. Critical nuclear localization signals (NLSs) of PITX2B were identified. A. The expression level of PITX2B in NLS mutant cell clones was determined by a Western blot analysis. PITX2B-mut-17 and -23: single-cell clones with double NLS mutations; PITX2B-mut-Mix: mixed-cell clones with double NLS mutations. β-Tubulin served as a loading control. B. Cell morphology images of PITX2B NLS mutant and mock stable transfectants. Regardless of whether the NLS of PITX2B was mutated, the cell morphology was unchanged. C. Fluorescent images showing the cellular localization of *PITX2B*-EGFP containing the wild-type or mutant NLS. The cell nuclei were counterstained with DAPI. The image magnification is 1,000×. D. The percentages of *PITX2B*-EGFP-expressing cells based on the cellular localization of *PITX2B*-EGFP containing the wild-type or mutant NLS were calculated and are presented as the mean ± SD of three independent experiments.

expression of downstream target genes and then affect cell functions, including cell shape, migration, and proliferation [12]. To further investigate whether the different cellular localizations of PITX2B could affect its function, as demonstrated above, we analysed the possible NLS in the PITX2B protein by PredictNLS online software (https://www.rostlab.org/owiki/index.php/PredictNLS). Two NLSs were identified in the PITX2B protein, and a site-directed mutagenesis assay was performed to construct single or double NLS mutant *PITX2B* expression vectors. Subsequently, we examined the total protein levels in the transfected cells using a Western blot analysis. The results showed that mutating both NLSs did not affect the total PITX2 expression levels (**Figure 3A**). In addition, the mutation status of the NLSs in the PITX2B protein did not change the cellular morphology compared with that of the mock control cells (**Figure 3B**). As expected, the PITX2B protein was predominantly localized in the nucleus of the wild-type *PITX2B*-EGFP-expressing cells. However, in the single NLS mutant construct-expressing cells (expressing PITX2B-R84P or PITX2B-R137P), the PITX2B protein could shuttle between the nucleus and cytoplasm. Furthermore, mutation in both NLSs resulted in markedly increased cytoplasmic localization and decreased nuclear expression of the PITX2B protein (**Figure 3C** and **3D**). Then, we determined whether these two NLSs of PITX2B

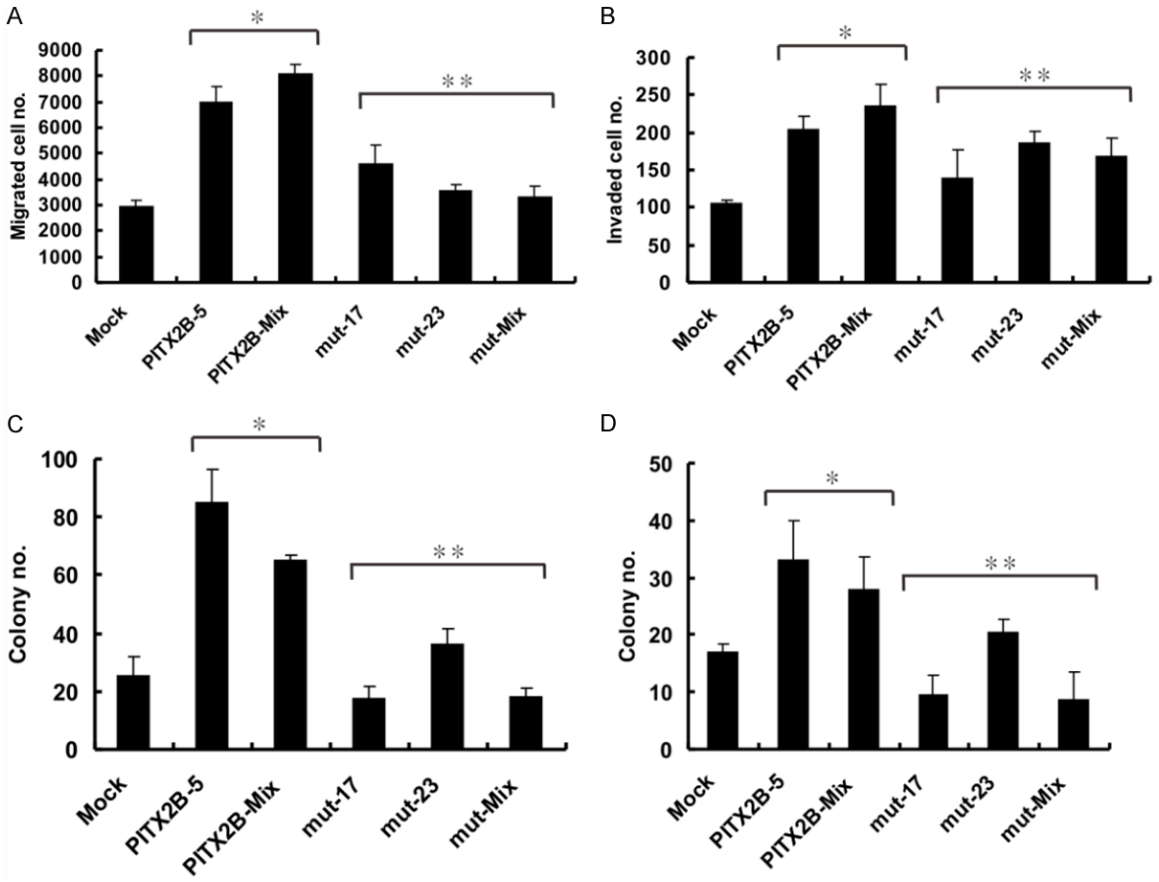

Figure 4. Nuclear localization signals (NLSs) are important for the oncogenic functions of PITX2B in lung cancer cells. A. The migration ability of PITX2B NLS mutant and mock transfectants was assessed by a scratch wound healing assay. B. The invasiveness of the PITX2B NLS mutant and mock transfectants was evaluated by Transwell assays. C. Anchorage-dependent colony formation assay of PITX2B NLS mutant and mock transfectants. D. The anchorage-independent colony formation of the PITX2B NLS mutant and mock transfectants was examined by a soft agar assay. All results are presented as the mean ± SD of three independent experiments. $^{*}P<0.05$ compared with the mock group. $^{**}P<0.05$ compared with the PITX2B-Mix group.

were important for its function. Our results show that mutating the NLSs of the PITX2B protein significantly decreased its oncogenic effects on migration, invasion, and anchorage-dependent and anchorage-independent colony formation capabilities in cancer cells (**Figure 4**). Our data suggest that these two NLSs are critical for PITX2B oncogenic function in lung cancer cells.

PITX2B knockdown induces autophagy in lung cancer cells

To evaluate the functional effect of the reduced *PITX2B* expression in lung cancer cells, we first examined the endogenous mRNA and protein expression levels of *PITX2B* in CL1-5 cells with high *PITX2B* expression after *PITX2*-specific or scramble siRNA transfection by qRT-PCR and Western blot analyses, respectively. As shown in **Figure 5A**, the *PITX2*-specific siRNA significantly reduced the mRNA expression level of *PITX2B* by 65%. In addition, the *PITX2*-specific siRNA efficiently decreased the endogenous protein expression levels compared with the scramble control siRNA (**Figure 5B**). To investigate the potential effects of *PITX2B* knockdown on cancer cell growth, CL1-5 cells were transfected with *PITX2*-specific or scramble siRNA, and a trypan blue exclusion assay was used to examine the cell viability. We found that the *PITX2*-specific siRNA significantly decreased the cell numbers compared with the scramble control 24 h post transfection. Interestingly, after 72 h of incubation, the viability of the *PITX2B*-knockdown CL1-5 cells was further

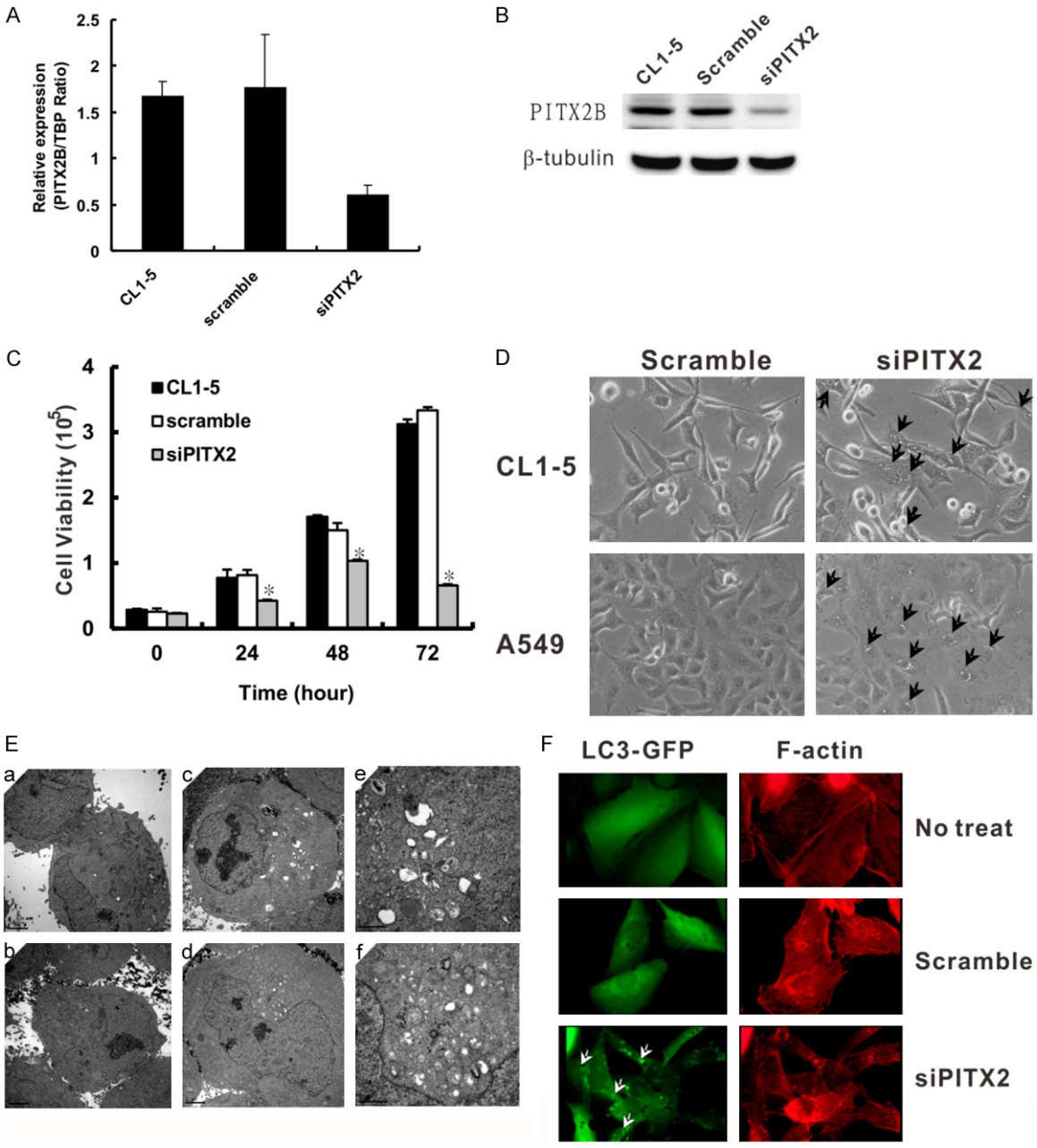

Figure 5. *PITX2B* knockdown induces autophagy in lung cancer cells. The silencing efficacy of the *PITX2*-specific siRNA was determined by (A) real-time quantitative RT-PCR and (B) a Western blot analysis using an anti-PITX2 antibody. β-Tubulin served as a loading control. (C) The viability of CL1-5 cells transfected with scramble siRNA (scramble) or *PITX2*-specific siRNA was evaluated by trypan blue exclusion assays at the indicated time. $^*P<0.05$ compared with the scramble siRNA control. The data are presented as the mean ± SD of three independent experiments. (D) Morphological changes (black arrowheads) were observed after *PITX2B* knockdown for 48 h in CL1-5 and A549 cells by inverted microscopy. (E) CL1-5 cells were transiently transfected with scramble siRNA (a, b) or *PITX2*-specific siRNAs (c-f) for 48 h, and then, the formation of autophagosomes in these cells was observed by TEM (a-d: magnification, ×5,000; scale bars, 2 μm. e and f: magnification, ×15,000; scale bars, 1 μm). (F) BEAS2B-EGFP-LC3 cells were transiently transfected with scramble or *PITX2*-specific siRNA for 48 h, and then, GFP-LC3 puncta (white arrowheads) were observed under a fluorescence microscope. The cells were fixed and stained with TRITC-phalloidin to visualize F-actin (red).

reduced to 19.8% of that of the scramble control cells (**Figure 5C**).

The morphological observation further revealed that the *PITX2B* knockdown decreased the cell

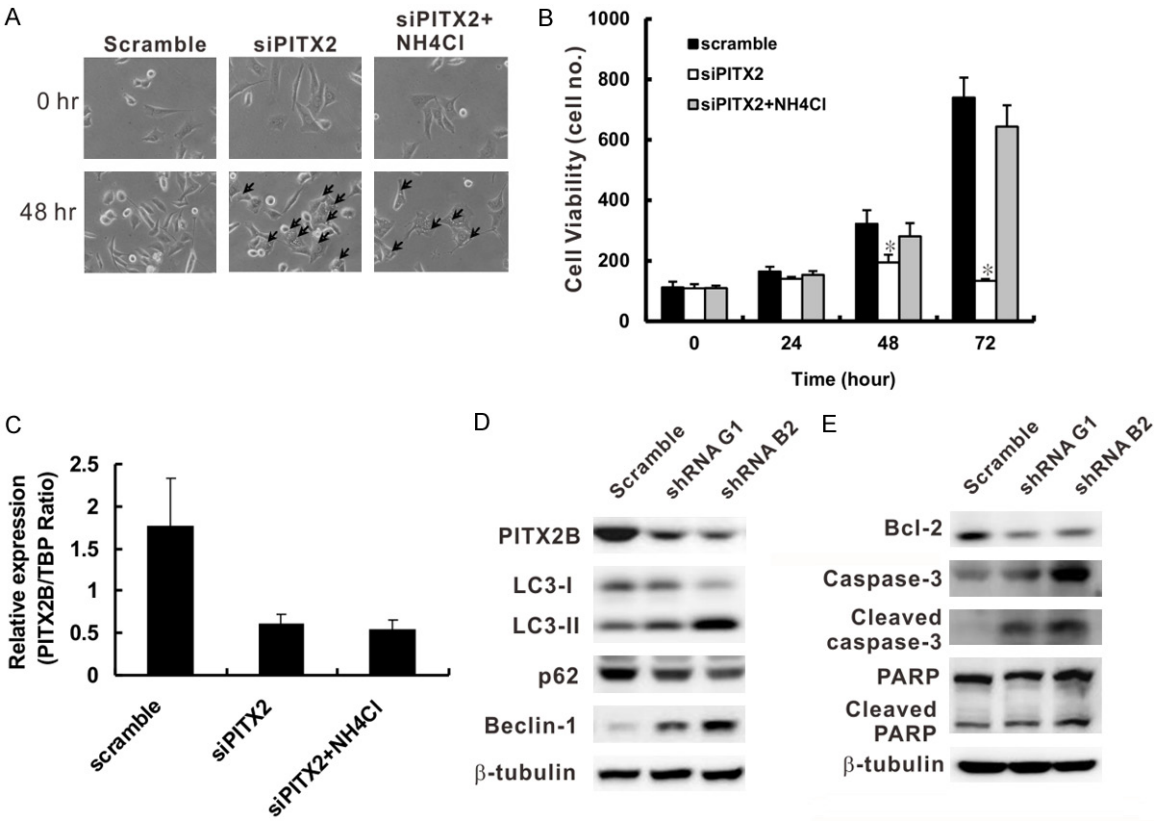

Figure 6. Autophagy and apoptotic cell death induction in *PITX2B*-knockdown lung cancer cells. A. CL1-5 cells were treated with 100 μM NH_4Cl after transfection with scramble or *PITX2*-specific siRNA for 24 h. Morphological changes (black arrowheads) were observed by inverted microscopy. NH_4Cl decreased the autophagy induced by *PITX2B* knockdown. B. The viability of CL1-5 cells transfected with scramble or *PITX2*-specific siRNA followed by NH_4Cl treatment was evaluated by trypan blue exclusion assays at the indicated time points. **P*<0.05 compared with the scramble control. The data are presented as the mean ± SD of three independent experiments. C. The mRNA expression level of *PITX2B* in CL1-5 cells transfected with scramble or *PITX2*-specific siRNA followed by NH_4Cl treatment was measured by real-time quantitative RT-PCR. D. Western blot analysis was carried out to detect the LC3, p62, and Beclin-1 protein levels after *PITX2*-specific or scramble shRNA transfection. Blots were re-probed with anti-β-tubulin as a loading control. E. Protein lysates of CL1-5 cells transfected with scramble or *PITX2*-specific shRNAs were harvested. The protein expression levels were measured by a Western blot analysis using antibodies against Bcl-2, Caspase-3, and PARP. β-Tubulin served as a loading control.

density (data not shown). Interestingly, we observed many vacuoles in the cytoplasm of the *PITX2B*-knockdown CL1-5 and A549 cells as shown in **Figure 5D**, which prompted us to investigate whether the *PITX2B* knockdown could induce autophagy in lung cancer cells. TEM was used to observe the formation of autophagosomes in *PITX2B*-knockdown cells. The images are shown in **Figure 5E**. Only a few vacuoles were observed in the scramble control cells (**Figure 5Ea**, **5Eb**); however, the knockdown of *PITX2B* resulted in the accumulation of autophagic vacuoles (**Figure 5Ec-f**), which exhibited autophagosomal and/or autolysosomal characteristics. In addition, to monitor autophagosome formation, we transiently transfected *PITX2*-specific or scramble siRNA into BEAS2B-EGFP-LC3 cells and obtained fluorescence images after 48 h. The results showed that the number of GFP-LC3 punctate dots per cell was increased after the *PITX2B* knockdown (**Figure 5F**).

Autophagy and cell death induction in PITX2B-knockdown lung cancer cells

Previous studies have demonstrated that autophagy plays dual roles in cell survival and cell death [22]; therefore, we investigated the role of autophagy in *PITX2B*-knockdown lung cancer cells. To show that the *PITX2B* knockdown induced late-stage autophagy, we first introduced NH_4Cl, which is a well-known lysosomal inhibitor that blocks lysosomal protein

degradation [37]. The results showed that the numbers of acidic vesicles were obviously increased in the *PITX2B*-knockdown group, whereas this effect was inhibited by the NH_4Cl treatment (**Figure 6A**). After the NH_4Cl treatment, the reduced viability of the *PITX2B*-knockdown cells was restored to a level almost equal to that of the scramble control cells (**Figure 6B**). These results indicate that autophagy induced by *PITX2B* knockdown could lead to cell death in lung cancer cells and that this effect could be reversed by lysosomal inhibitor treatment.

To rule out the possibility that the increased cell viability was due to changes in the expression levels of *PITX2B* induced by the NH_4Cl treatment, we examined the *PITX2B* mRNA expression levels after the NH_4Cl treatment. The results showed that the *PITX2B* mRNA expression level was unchanged in *PITX2B*-knockdown cells with or without the NH_4Cl treatment (**Figure 6C**). The autophagy-specific markers Beclin-1, p62 and LC3 were used to examine the autophagic flux and autophagic levels by a Western blot analysis. The observed increased conversion of LC3-I/II, the downregulation of p62 expression and the upregulation of Beclin-1 expression demonstrated an increased formation of autophagosomes after the *PITX2B* knockdown (**Figure 6D**). To further confirm that cell death induced by *PITX2B* knockdown is related to apoptosis, the expression levels of apoptosis-related proteins, including caspase-3, Bcl-2, and PARP, were examined by a Western blot analysis. The results showed that compared with scramble control cells, the *PITX2B* knockdown increased the cleaved caspase-3 and PARP levels but decreased the levels of the antiapoptotic protein Bcl-2 in the *PITX2B*-knockdown cells (**Figure 6E**). Collectively, these results demonstrate that *PITX2B* knockdown in lung cancer cells could induce autophagy and ultimately cause tumour cell death.

PITX2 expression is associated with the clinical outcomes of early-stage NSCLC patients

Although our results suggest that *PITX2B* plays oncogenic roles *in vivo* and *in vitro*, such data may not fully reflect clinical malignancy. We extended our analysis by examining the *PITX2B* expression levels in tumour specimens from 98 and 736 patients with early-stage NSCLC in a Taiwanese cohort and GEO datasets, respectively. The clinical characteristics of the patients are summarized in Supplementary Table 1. The survival analyses of 736 patients with stage I and II NSCLC indicated that the patients with high *PITX2* expression levels showed a reduced overall survival (P=0.003, **Figure 7A**). Moreover, the analysis of 568 patients with stage I NSCLC revealed that the patients with a high expression of *PITX2* were associated with a reduced overall survival (P=0.002, **Figure 7B**). Furthermore, the analyses of the 98 Taiwanese patients with early-stage NSCLC consistently showed that the patients with a high expression of *PITX2* exhibited a significantly reduced overall survival time (stage I and II, P=0.039, **Figure 7C**; stage I, P=0.017, **Figure 7D**, respectively). Similarly, a high gene expression level of PITX2 predicted a poor clinical outcome in Taiwanese patients with early-stage lung adenocarcinoma (stage I and II, P=0.041, **Figure 7E**; stage I, P=0.003, **Figure 7F**). A multivariate Cox proportional hazards regression analysis with the covariates sex and age was used to assess the independent prognostic factors in the recruited cohort (n=98) and the published cohort (n=736). After considering the effects of the covariates, all hazard ratios of the *PITX2* expression level were still significant (**Table 1**). These results show that PITX2 could play an oncogenic role in the clinical prognosis of patients with early-stage NSCLC.

Discussion

Tumour progression is a multistage process that renders cancer a more aggressive and malignant phenotype. A higher tumour grade indicates a more advanced status characterized by higher invasiveness and cell proliferation capabilities [38]. A recent report suggested that *PITX2* could enhance lung adenocarcinoma progression; however, the data did not clarify which isoform of *PITX2* was explored [17]. In this study, we first identified *PITX2B* as the major isoform of *PITX2* in human lung adenocarcinoma cells. The expression of *PITX2B* was positively correlated with not only cancer cell invasiveness but also a poor outcome in early-stage NSCLC patients. Given the important role of *PITX2B* in NSCLC cell invasiveness and clinical outcomes, we focused on the func-

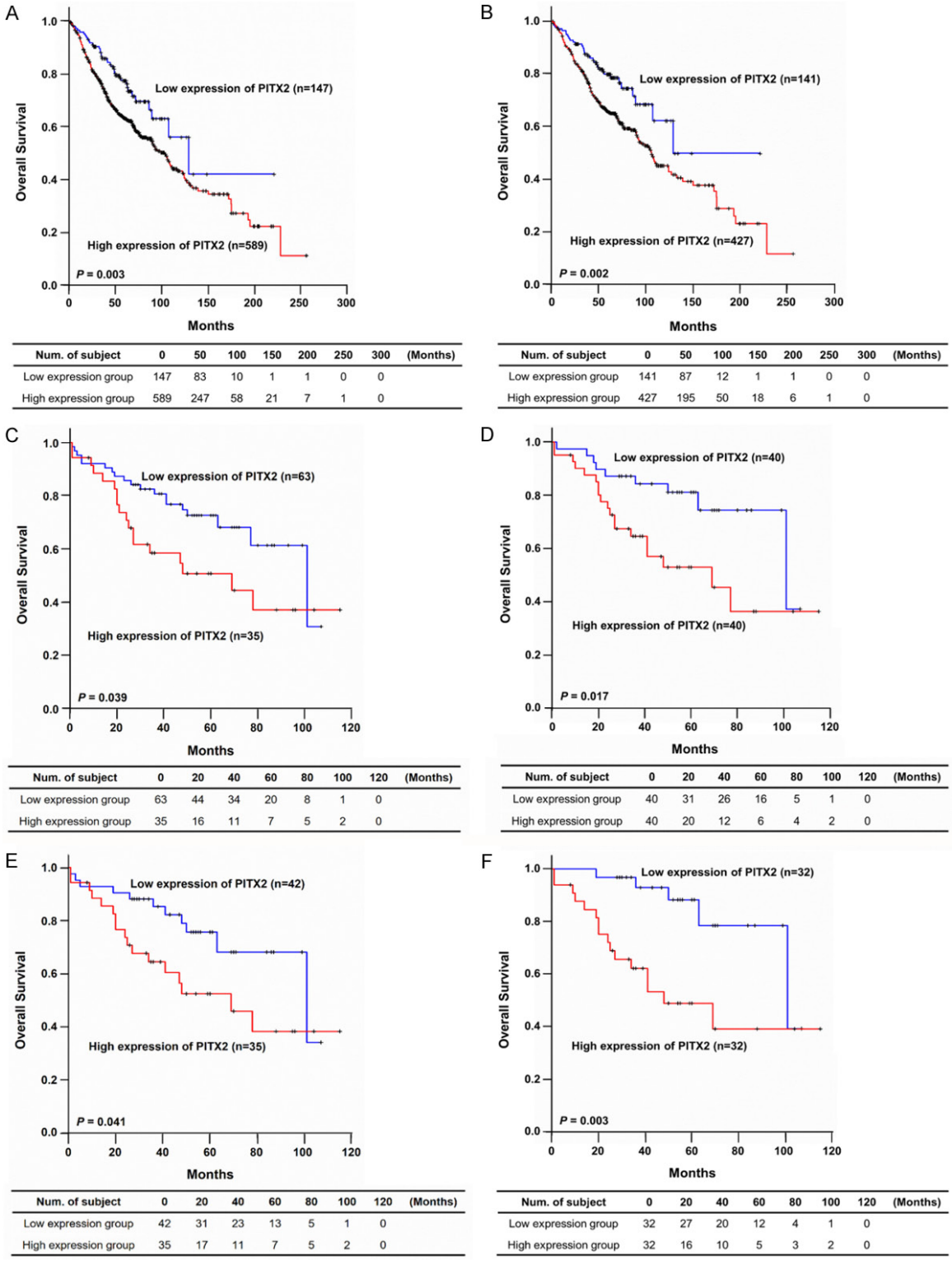

Num. of subject	0	50	100	150	200	250	300	(Months)
Low expression group	147	83	10	1	1	0	0	
High expression group	589	247	58	21	7	1	0	

Num. of subject	0	50	100	150	200	250	300	(Months)
Low expression group	141	87	12	1	1	0	0	
High expression group	427	195	50	18	6	1	0	

Num. of subject	0	20	40	60	80	100	120	(Months)
Low expression group	63	44	34	20	8	1	0	
High expression group	35	16	11	7	5	2	0	

Num. of subject	0	20	40	60	80	100	120	(Months)
Low expression group	40	31	26	16	5	1	0	
High expression group	40	20	12	6	4	2	0	

Num. of subject	0	20	40	60	80	100	120	(Months)
Low expression group	42	31	23	13	5	1	0	
High expression group	35	17	11	7	5	2	0	

Num. of subject	0	20	40	60	80	100	120	(Months)
Low expression group	32	27	20	12	4	1	0	
High expression group	32	16	10	5	3	2	0	

Figure 7. Kaplan-Meier estimates of the overall survival of patients with early-stage NSCLC according to the *PITX2* expression level. Overall survival curves were generated based on the *PITX2* expression level as measured by published NSCLC microarray data and RT-PCR. For the published microarray datasets, the overall survival curves of (A) 736 patients with stage I and II NSCLC and (B) 568 patients with stage I disease are shown. In the independent Taiwanese cohort, the overall survival curves of (C) 98 patients with stage I and II NSCLC and (D) 80 patients with stage I disease are shown. The overall survival curves of (E) 77 Taiwanese patients with stage I and II lung adenocarcinoma and (F) 64 patients in this cohort who had stage I disease are also shown. The survival curves were estimated by the Kaplan-Meier method, and statistical significance was evaluated by the log-rank test. *P*-values less than 0.05 were considered statistically significant.

Table 1. Multivariate Cox regression model of PITX2 in the overall survival of patients with early-stage NSCLC

Variable	Hazard ratio	95% HR C.I.		*P*-value
Patients with stage I and II NSCLC in the microarray datasets (n=736)				
PITX2	1.56	1.10	2.23	0.013
Gender	1.24	0.97	1.59	0.083
Age	1.04	1.02	1.05	<0.0001
Patients with stage I NSCLC in the microarray datasets (n=568)				
PITX2	1.69	1.14	2.50	0.009
Gender	1.28	0.95	1.73	0.099
Age	1.05	1.03	1.06	<0.0001
Patients with stage I and II NSCLC in the Taiwanese cohort (n=98)				
PITX2	2.28	1.18	4.40	0.014
Gender	2.89	1.24	6.71	0.014
Age	0.99	0.97	1.02	0.694
Patients with stage I NSCLC in the Taiwanese cohort (n=80)				
PITX2	2.65	1.18	5.93	0.018
Gender	2.53	0.96	6.67	0.061
Age	0.99	0.97	1.02	0.704
Patients with stage I and II lung adenocarcinoma in the Taiwanese cohort (n=77)				
PITX2	2.22	1.03	4.78	0.041
Gender	2.61	1.10	6.21	0.030
Age	1.00	0.97	1.02	0.845
Patients with stage I lung adenocarcinoma in the Taiwanese cohort (n=64)				
PITX2	4.38	1.58	12.12	0.004
Gender	2.55	0.92	7.06	0.071
Age	1.00	0.97	1.03	0.954

tional roles of *PITX2B* in lung adenocarcinoma cells, which have not been reported thus far. Both the *in vitro* and *in vivo* studies revealed that PITX2B promotes cancer cell migration, invasion, colony formation ability and tumour growth in a tumour xenograft mouse model. These results are consistent with previously published reports showing that PITX2 could promote carcinogenesis in ovarian and thyroid cancer [13, 16]. However, this study is the first to demonstrate that PITX2B can contribute to lung cancer progression. In addition, our study shows that the expression levels of *PITX2B* were increased in lung cancer, particularly in highly invasive cells, indicating that *PITX2B* may play a critical role in driving aggressive phenotypes in lung cancer. Several genes or molecules have been suggested to be involved in *PITX2*-mediated tumour progression. For example, genes associated with the Wnt/beta-Catenin signalling pathway have been discovered in breast, thyroid, and lung cancers [17, 39, 40]. In addition, miR-21 and miR-644a have been found to regulate the expression levels of *PITX2* in pituitary adenoma and oesophageal squamous cell carcinoma cells, respectively [41, 42]. However, the molecular mechanisms underlying *PITX2B* expression and functions in lung cancer need to be further investigated in the future.

Our analysis shows that a higher *PITX2B* mRNA expression is associated with a shorter overall survival in early-stage NSCLC patients, including both stage I patients from a Taiwanese cohort and published GEO datasets. More importantly, *PITX2B* expression also predicted a poor clinical outcome in Taiwanese patients with early-stage lung adenocarcinoma. Because many distinct characteristics differ between the two major lung cancer subtypes, i.e., adenocarcinoma and squamous cell carcinoma, different molecular markers need to be developed to sensitively detect these two types of lung cancer [5]. Many DNA methylation markers of these two types of lung cancer have been

developed [5, 6]. PITX2 was identified as a DNA methylation marker in an eight-gene panel of squamous cell lung cancers [5]. Taken together, our results suggest that *PITX2B* could serve as a suitable prognostic biomarker of early-stage NSCLC.

PITX2 has been known to play an important role in determining left-right asymmetry and the development of multiple organs [8]. For example, left identity was found to be mediated by the Nodal-Pitx2 axis, which is inhibited by Snail, an epithelial-mesenchymal transition (EMT) inducer, on the right-hand side in vertebrates [43]. In addition, PRRX1 knockdown-induced PITX2 upregulation represses Slug transcriptional activities and increases E-cadherin expression levels in hepatocellular carcinoma cells [44]. Our cell morphology observations showed that the PITX2B-overexpressing cells had spindle shapes; whether PITX2B could regulate EMT signalling in lung cancer could be worth investigating in future studies.

As a transcription factor, PITX2B can activate and/or repress the transcription of its target genes to perform specific cellular functions. Our data demonstrate that the oncogenic characteristics of PITX2B are mediated through two important NLSs located at amino acids 80 to 91 and 134 to 146. When the NLS structures of PITX2B were changed by two point mutations, namely, R84P and R137P, the cytoplasmic localization of PITX2B was increased, and the nuclear expression of the PITX2B protein was restricted. In addition, lung cancer cells expressing PITX2B NLS mutant proteins lost their effects on increasing migration, invasion and colony formation capabilities compared to wild-type NLS control cells (**Figure 3**). To the best of our knowledge, this study is the first to identify critical NLSs of PITX2B in lung cancer progression. These results suggest that designing or identifying molecules or proteins that target the PITX2B protein in the cytoplasm and prevent its entry into the nucleus could be an efficient therapeutic strategy for lung cancer. Some PITX2-interacting proteins have been identified, including the HPV E6 protein [45]. Previous studies suggest that *PITX2A* could interfere with *E6/E6AP*-mediated p53 degradation by binding the E6 protein, leading to the accumulation of functional p53 protein in HeLa cells [45]. Thus, our hypothesis needs to be investigated in the future.

To confirm the functional effect of the reduced *PITX2B* expression in lung cancer cells, we performed *PITX2*-specific siRNA or shRNA knockdown experiments in CL1-5 cells with high *PITX2B* expression. We found that the knockdown of *PITX2B* could reduce lung cancer cell viability to 19.8% after 72 h of transfection with *PITX2*-specific siRNA. In addition, our data show that the knockdown of *PITX2B* could reduce the expression of the antiapoptotic protein Bcl-2 and increase the expression levels of proapoptotic proteins, including cleaved caspase 3 and PARP. These results are consistent with a previous study showing that the knockdown of *PITX2* could decrease cell viability via the induction of an apoptotic mechanism involving the activation of executioner caspase activity in gonadotroph cells [14]. A recent study also showed that the knockdown of *PITX2* could lead to G1/S cell cycle arrest and a higher apoptotic ratio in H1299 lung cancer cells [17]. However, in oesophageal squamous cell carcinoma (ESCC) cell lines, the knockdown of *PITX2* did not appear to induce cell apoptosis [46]. Therefore, the differential effects of *PITX2* knockdown could be associated with the specific *PITX2* isoform targeted and/or tissue specificity.

More interestingly, for the first time, we demonstrate that the knockdown of *PITX2B* could induce autophagy in the NSCLC cell lines CL1-5 and A549. First, the occurrence of autophagy was demonstrated by TEM, which is considered the standard technology for the morphological evaluation of autophagy [47]. In addition, our data revealed that the knockdown of *PITX2B* could stimulate the conversion of LC3-I to LC3-II and increase the number of GFP-LC3 puncta in BEAS2B cells. Moreover, a well-known lysosomal inhibitor, i.e., NH_4Cl, that blocks lysosomal protein degradation could reduce autophagy and restore cell viability to levels similar to those observed in scramble siRNA transfectants. Furthermore, autophagy was investigated at the molecular level by biochemical methods. Our results indicate that the levels of both Beclin-1 and LC3-II, which are considered markers of autophagy, are significantly increased after *PITX2B* knockdown in CL1-5 cells, which was accompanied by the downregulation of p62 expression. Altogether, these results indicate that autophagy is induced by *PITX2B* knockdown. Autophagy is a catabolic process regulated by a series of Atg proteins in which

unnecessary by-products and damaged organelles are engulfed into doubled-membrane vesicles termed autophagosomes and subsequently transported to lysosomes [48, 49]. Loaded autophagosomes fuse with lysosomes to form autolysosomes, where cargoes are degraded by lysosomal enzymes and recycled [49]. According to our findings, we propose that *PITX2B* knockdown can drive lung cancer cells to initiate the autophagy process until autolysosome formation. In the absence of a lysosomal inhibitor, *PITX2B* knockdown could complete the autophagic process and ultimately lead to cell death. However, currently, the molecular mechanism underlying *PITX2B* knockdown-induced autophagy is incompletely understood and requires further study.

Recent studies have noted the conflicting roles of autophagy in cancer progression and response to therapy [50]. This discrepancy appears to highly depend on the cell types and inducers [51, 52]. In our study, we investigated the relationship between autophagy and apoptosis in *PITX2B*-depleted NSCLC cells and found that following the NH_4Cl treatment, the viability of the *PITX2B*-knockdown cells was significantly recovered. Previous studies have demonstrated that antiapoptotic Bcl-2 family members can form complexes with Beclin-1 and prevent it from promoting autophagy [53, 54]. Our data show that the *PITX2B* knockdown could enhance apoptosis through the upregulation of the expression of proapoptotic proteins and downregulation of the expression of antiapoptotic proteins, such as Bcl-2. Taken together, these results suggest that autophagy induced by *PITX2B* knockdown contributes to promoting apoptosis in human NSCLC cells.

In conclusion, we show that the overexpression of *PITX2B* could enhance cancer cell migration, invasion, and colony formation capabilities *in vitro* and tumorigenesis *in vivo*. In addition, we demonstrate that a high *PITX2B* expression is associated with a poor overall survival in early-stage NSCLC patients. Moreover, our data indicate that the knockdown of *PITX2B* could induce autophagy in human NSCLC cells and that cell death decreases when autophagy is inhibited by the lysosomal inhibitor NH_4Cl. Altogether, these findings suggest that the knockdown of *PITX2B* is a promising novel chemotherapeutic strategy for the treatment of human non-small-cell lung carcinoma.

Acknowledgements

This work was supported by grants from the Ministry of Science and Technology, Taiwan, R.O.C. (NSC99-2628-B-030-002-MY3, MOST 103-2320-B-005-005-MY3, and MOST107-2314-B-030-010-MY2). The funders had no role in the study design, data collection and analysis, decision to publish, or preparation of the manuscript. The authors thank the Electron Microscope Laboratory of Prof Tzong Jwo Jang at the School of Medicine, Fu Jen Catholic University, New Taipei, Taiwan for technical assistance. We also thank Prof Jeng Jer Shieh at the Institute of Biomedical Sciences, National Chung Hsing University, Taichung, Taiwan for providing the BEAS2B-EGFP-LC3 cells.

Disclosure of conflicts of interest

None.

Address correspondence to: Jeremy JW Chen, Institute of Biomedical Sciences, National Chung Hsing University, No. 145, Xingda Road, South District, Taichung, Taiwan. Tel: +886-4-22840896 Ext. 125; Fax: +886-4-22853469; E-mail: jwchen@dragon.nchu.edu.tw

References

[1] Hsin IL, Ou CC, Wu TC, Jan MS, Wu MF, Chiu LY, Lue KH and Ko JL. GMI, an immunomodulatory protein from Ganoderma microsporum, induces autophagy in non-small cell lung cancer cells. Autophagy 2011; 7: 873-882.

[2] Mikeska T, Bock C, Do H and Dobrovic A. DNA methylation biomarkers in cancer: progress towards clinical implementation. Expert Rev Mol Diagn 2012; 12: 473-487.

[3] Siegel RL, Ma J, Zou Z and Jemal A. Cancer statistics, 2014. CA Cancer J Clin 2014; 64: 9-29.

[4] Siegel RL, Miller KD and Jemal A. Cancer statistics, 2019. CA Cancer J Clin 2019; 69: 7-34.

[5] Anglim PP, Galler JS, Koss MN, Hagen JA, Turla S, Campan M, Weisenberger DJ, Laird PW, Siegmund KD and Laird-Offringa IA. Identification of a panel of sensitive and specific DNA methylation markers for squamous cell lung cancer. Mol Cancer 2008; 7: 62.

[6] ZhaoY, Zhou H, Ma K, Sun J, Feng X, Geng J, Gu J, Wang W, Zhang H, He Y, Guo S, Zhou X, Yu J and Lin Q. Abnormal methylation of seven genes and their associations with clinical characteristics in early stage non-small cell lung cancer. Oncol Lett 2013; 5: 1211-1218.

[7] Hjalt TA, Semina EV, Amendt BA and Murray JC. The Pitx2 protein in mouse development. Dev Dyn 2000; 218: 195-200.

[8] Lin CR, Kioussi C, O'Connell S, Briata P, Szeto D, Liu F, Lzpisúa-Belmonte JC and Rosenfeld MG. Pitx2 regulates lung asymmetry, cardiac positioning, and pituitary and tooth morphogenesis. Nature 1999; 401: 279-282.
[9] Amendt BA, Semina EV and Alward WL. Rieger syndrome: a clinical, molecular, and biochemical analysis. Cell Mol Life Sci 2000; 57: 1652-1666.
[10] Cox CJ, Espinoza HM, McWilliams B, Chappell K, Morton L, Hjalt TA, Semina EV and Amendt BA. Differential regulation of gene expression by PITX2 isoforms. J Biol Chem 2002; 277: 25001-25010.
[11] Semina EV, Reiter R, Leysens NJ, Alward WL, Small KW, Datson NA, Siegel-Bartelt J, Bierke-Nelson D, Bitoun P, Zabel BU, Carey JC and Murray JC. Cloning and characterization of a novel bicoid-related homeobox transcription factor gene, RIEG, involved in Rieger syndrome. Nat Genet 1996; 14: 392-399.
[12] Wei Q and Adelstein RS. Pitx2a expression alters actin-myosin cytoskeleton and migration of HeLa cells through Rho GTPase signaling. Mol Biol Cell 2002; 13: 683-697.
[13] Fung FK, Chan DW, Liu VW, Leung TH, Cheung AN and Ngan HY. Increased expression of PITX2 transcription factor contributes to ovarian cancer progression. PLoS One 2012; 7: e37076.
[14] Acunzo J, Roche C, Defilles C, Thirion S, Quentien MH, Figarella-Branger D, Graillon T, Dufour H, Brue T, Pellegrini I, Enjalbert A and Barlier A. Inactivation of PITX2 transcription factor induced apoptosis of gonadotroph tumoral cells. Endocrinology 2011; 52: 3884-3892.
[15] Hirose H, Ishii H, Mimori K, Tanaka F, Takemasa I, Mizushima T, Ikeda M, Yamamoto H, Sekimoto M, Doki Y and Mori M. The significance of PITX2 overexpression in human colorectal cancer. Ann Surg Oncol 2011; 18: 3005-3012.
[16] Huang Y, Guigon CJ, Fan J, Cheng SY and Zhu GZ. Pituitary homeobox 2 (PITX2) promotes thyroid carcinogenesis by activation of cyclin D2. Cell Cycle 2010; 9: 1333-1341.
[17] Luo J, Yao Y, Ji S, Sun Q, Xu Y, Liu K, Diao Q, Qiang Y and Shen Y. PITX2 enhances progression of lung adenocarcinoma by transcriptionally regulating WNT3A and activating Wnt/β-catenin signaling pathway. Cancer Cell Int 2019; 19: 96.
[18] Zirn B, Hartmann O, Samans B, Krause M, Wittmann S, Mertens F, Graf N, Eilers M and Gessler M. Expression profiling of Wilms tumors reveals new candidate genes for different clinical parameters. Int J Cancer 2006; 118: 1954-1962.
[19] Høyer-Hansen M and Jäättelä M. Autophagy: an emerging target for cancer therapy. Autophagy 2008; 4: 574-580.
[20] Klionsky DJ. Autophagy: from phenomenology to molecular understanding in less than a decade. Nat Rev Mol Cell Biol 2007; 8: 931-937.
[21] Levine B and Klionsky DJ. Development by self-digestion: molecular mechanisms and biological functions of autophagy. Dev Cell 2004; 6: 463-477.
[22] Kondo Y, Kanzawa T, Sawaya R and Kondo S. The role of autophagy in cancer development and response to therapy. Nat Rev Cancer 2005; 5: 726-734.
[23] Chen JJW, Peck K, Hong TM, Yang SC, Sher YP, Shih JY, Wu R, Cheng JL, Roffler SR, Wu CW and Yang PC. Global analysis of gene expression in invasion by a lung cancer model. Cancer Res 2001; 61: 5223-5230.
[24] Brierley JD, Gospodarowicz MK and Wittekind C. The TNM classification of malignant tumours. 8th ed. Hoboken (NJ): Wiley-Blackwell; 2016.
[25] Tsai MF, Wang CC, Chang GC, Chen CY, Chen HY, Cheng CL, Yang YP, Wu CY, Shih FY, Liu CC, Lin HP, Jou YS, Lin SC, Lin CW, Chen WJ, Chan WK, Chen JJW and Yang PC. A new tumor suppressor DnaJ-like heat shock protein, HLJ1, and survival of patients with non-small-cell lung carcinoma. J Natl Cancer Inst 2006; 98: 825-838.
[26] Rousseaux S, Debernardi A, Jacquiau B, Vitte AL, Vesin A, Nagy-Mignotte H, Moro-Sibilot D, Brichon PY, Lantuejoul S, Hainaut P, Laffaire J, de Reyniès A, Beer DG, Timsit JF, Brambilla C, Brambilla E and Khochbin S. Ectopic activation of germline and placental genes identifies aggressive metastasis-prone lung cancers. Sci Transl Med 2013; 5: 186ra166.
[27] Botling J, Edlund K, Lohr M, Hellwig B, Holmberg L, Lambe M, Berglund A, Ekman S, Bergqvist M, Pontén F, André K, Fernandes O, Karlsson M, Helenius G, Karlsson C, Rahnenführer J, Hengstler JG and Micke P. Biomarker discovery in non-small cell lung cancer: integrating gene expression profiling, meta-analysis, and tissue microarray validation. Clin Cancer Res 2013; 19: 194-204.
[28] Jabs V, Edlund K, Konig H, Grinberg M, Madjar K, Rahnenfuhrer J, Ekman S, Bergkvist M, Holmberg L, Ickstadt K, Botling J, Hengstler JG and Micke P. Integrative analysis of genome-wide gene copy number changes and gene expression in non-small cell lung cancer. PLoS One 2017; 12: e0187246.
[29] Lohr M, Hellwig B, Edlund K, Mattsson JS, Botling J, Schmidt M, Hengstler JG, Micke P and Rahnenführer J. Identification of sample annotation errors in gene expression datasets. Arch Toxicol 2015; 89: 2265-2272.

[30] Xie Y, Xiao G, Coombes KR, Behrens C, Solis LM, Raso G, Girard L, Erickson HS, Roth J, Heymach JV, Moran C, Danenberg K, Minna JD and Wistuba II. Robust gene expression signature from formalin-fixed paraffin-embedded samples predicts prognosis of non-small-cell lung cancer patients. Clin Cancer Res 2011; 17: 5705-5714.

[31] Okayama H, Kohno T, Ishii Y, Shimada Y, Shiraishi K, Iwakawa R, Furuta K, Tsuta K, Shibata T, Yamamoto S, Watanabe S, Sakamoto H, Kumamoto K, Takenoshita S, Gotoh N, Mizuno H, Sarai A, Kawano S, Yamaguchi R, Miyano S and Yokota J. Identification of genes upregulated in ALK-positive and EGFR/KRAS/ALK-negative lung adenocarcinomas. Cancer Res 2012; 72: 100-111.

[32] Yamauchi M, Yamaguchi R, Nakata A, Kohno T, Nagasaki M, Shimamura T, Imoto S, Saito A, Ueno K, Hatanaka Y, Yoshida R, Higuchi T, Nomura M, Beer DG, Yokota J, Miyano S and Gotoh N. Epidermal growth factor receptor tyrosine kinase defines critical prognostic genes of stage I lung adenocarcinoma. PLoS One 2012; 7: e43923.

[33] Der SD, Sykes J, Pintilie M, Zhu CQ, Strumpf D, Liu N, Jurisica I, Shepherd FA and Tsao MS. Validation of a histology-independent prognostic gene signature for early-stage, non-small-cell lung cancer including stage IA patients. J Thorac Oncol 2014; 9: 59-64.

[34] Bolstad BM, Irizarry RA, Astrand M and Speed TP. A comparison of normalization methods for high density oligonucleotide array data based on variance and bias. Bioinformatics 2003; 19: 185-193.

[35] Quentien MH, Barlier A, Franc JL, Pellegrini I, Brue T and Enjalbert A. Pituitary transcription factors: from congenital deficiencies to gene therapy. J Neuroendocrinol 2006; 18: 633-642.

[36] Chu YW, Yang PC, Yang SC, Shyu YC, Hendrix MJ, Wu R and Wu CW. Selection of invasive and metastatic subpopulations from a human lung adenocarcinoma cell line. Am J Respir Cell Mol Biol 1997; 17: 353-360.

[37] Ahlberg J, Henell F and Glaumann H. Proteolysis in isolated autophagic vacuoles from rat liver. Effect of pH and of proteolytic inhibitors. Exp Cell Res 1982; 142: 373-383.

[38] Saad AF, Hu W and Sood AK. Microenvironment and pathogenesis of epithelial ovarian cancer. Horm Cancer 2010; 1: 277-290.

[39] Pillai SG, Dasgupta N, Siddappa CM, Watson MA, Fleming T, Trinkaus K and Aft R. Paired-like Homeodomain Transcription factor 2 expression by breast cancer bone marrow disseminated tumor cells is associated with early recurrent disease development. Breast Cancer Res Treat 2015; 153: 507-517.

[40] Liu Y, Huang Y and Zhu GZ. Cyclin A1 is a transcriptional target of PITX2 and overexpressed in papillary thyroid carcinoma. Mol Cell Biochem 2013; 384: 221-227.

[41] Cui M, Zhang M, Liu HF and Wang JP. Effects of microRNA-21 targeting PITX2 on proliferation and apoptosis of pituitary tumor cells. Eur Rev Med Pharmacol Sci 2017; 21: 2995-3004.

[42] Zhang JX, Chen ZH, Xu Y, Chen JW, Weng HW, Yun M, Zheng ZS, Chen C, Wu BL, Li EM, Fu JH, Ye S and Xie D. Downregulation of MicroRNA-644a promotes esophageal squamous cell carcinoma aggressiveness and stem cell-like phenotype via dysregulation of PITX2. Clin Cancer Res 2017; 23: 298-310.

[43] Patel K, Isaac A and Cooke J. Nodal signalling and the roles of the transcription factors SnR and Pitx2 in vertebrate left-right asymmetry. Curr Biol 1999; 9: 609-612.

[44] Chen W, Wu J, Shi W, Zhang G, Chen X, Ji A, Wang Z, Wu J and Jiang C. PRRX1 deficiency induces mesenchymal-epithelial transition through PITX2/miR-200-dependent SLUG/CTNNB1 regulation in hepatocellular carcinoma. Cancer Sci 2021; 112: 2158-2172.

[45] Wei Q. Pitx2a binds to human papillomavirus type 18 E6 protein and inhibits E6-mediated p53 degradation in HeLa cells. J Biol Chem 2005; 280: 37790-37797.

[46] Zhang JX, Tong ZT, Yang L, Wang F, Chai HP, Zhang F, Xie MR, Zhang AL, Wu LM, Hong H, Yin L, Wang H, Wang HY and Zhao Y. PITX2: a promising predictive biomarker of patients' prognosis and chemoradioresistance in esophageal squamous cell carcinoma. Int J Cancer 2013; 132: 2567-2577.

[47] Tanida I, Ueno T and Kominami E. LC3 conjugation system in mammalian autophagy. Int J Biochem Cell Biol 2004; 36: 2503-2518.

[48] Mizushima N. Autophagy: process and function. Genes Dev 2007; 21: 2861-2873.

[49] Xie Z and Klionsky DJ. Autophagosome formation: core machinery and adaptations. Nat Cell Biol 2007; 9: 1102-1109.

[50] Xi G, Hu X, Wu B, Jiang H, Young CY, Pang Y and Yuan H. Autophagy inhibition promotes paclitaxel-induced apoptosis in cancer cells. Cancer Lett 2011; 307: 141-148.

[51] Calfon M, Zeng H, Urano F, Till JH, Hubbard SR, Harding HP, Clark SG and Ron D. IRE1 couples endoplasmic reticulum load to secretory capacity by processing the XBP-1 mRNA. Nature 2002; 415: 92-96.

[52] Salazar M, Carracedo A, Salanueva IJ, Hernández-Tiedra S, Lorente M, Egia A, Vázquez P, Blázquez C, Torres S, Garcia S, Nowak J, Fimia GM, Piacentini M, Cecconi F, Pandolfi PP,

González-Feria L, Iovanna JL, Guzmán M, Boya P and Velasco G. Cannabinoid action induces autophagy-mediated cell death through stimulation of ER stress in human glioma cells. J Clin Invest 2009; 119: 1359-1372.

[53] Pattingre S, Tassa A, Qu X, Garuti R, Liang XH, Mizushima N, Packer M, Schneider MD and Levine B. Bcl-2 antiapoptotic proteins inhibit Beclin 1-dependent autophagy. Cell 2005; 122: 927-939.

[54] Erlich S, Mizrachy L, Segev O, Lindenboim L, Zmira O, Adi-Harel S, Hirsch JA, Stein R and Pinkas-Kramarski R. Differential interactions between Beclin 1 and Bcl-2 family members. Autophagy 2007; 3: 561-568.

Supplementary Table 1. Clinical characteristics of early-stage NSCLC patients

	Published cohort	Taiwan cohort
No. of patients	736	98
Age - yr	63.59±9.43	70.84±14.15
Gender - no. of patients (%)		
Male	417 (56.66)	66 (67.35)
Female	319 (43.34)	32 (32.65)
Tumor stage - no. of patients (%)		
I	568 (77.17)	80 (81.63)
II	168 (22.83)	18 (18.37)
Tumor type - no. of patients (%)		
Adenocarcinoma	565 (76.77)	77 (78.57)
Squamous cell carcinoma	171 (23.23)	21 (21.43)